

# In-vivo Measurement of Relationship between Applied Current Amplitude and Current Density Magnitude from 10 mA to 110 mA

Tim P. DeMonte, *Member, IEEE*, Dinghui Wang, Weijing Ma, Jia-Hong Gao, and Michael L. G. Joy, *Member, IEEE*

**Abstract**— Current density imaging (CDI) is a magnetic resonance imaging (MRI) technique used to quantitatively measure current density vectors throughout the volume of an object/subject placed in the MRI system. Electrical current pulses are applied externally to the object/subject and are synchronized with the MRI sequence. In this work, CDI is used to measure average current density magnitude in the torso region of an in-vivo piglet for applied current pulse amplitudes ranging from 10 mA to 110 mA. The relationship between applied current amplitude and current density magnitude is linear in simple electronic elements such as wires and resistors; however, this relationship may not be linear in living tissue. An understanding of this relationship is useful for research in defibrillation, human electro-muscular incapacitation (e.g. TASER®) and other bioelectric stimulation devices. This work will show that the current amplitude to current density magnitude relationship is slightly nonlinear in living tissue in the range of 10 mA to 110 mA.

## I. INTRODUCTION

CURRENT density imaging (CDI) is a technique based on magnetic resonance imaging (MRI) that can quantitatively measure the magnitude and direction of current density vectors throughout a volume of tissue [1]. The present technique is limited to measuring current density caused by externally applied electrical pulses synchronized with the MRI sequence. CDI has been demonstrated as a useful tool in studying defibrillation [2], human electro-muscular incapacitation (HEMI) (e.g. TASER®) devices [3] and numerous other bioelectric stimulation devices. This document reports on a recent study performed on in-vivo piglets that uses CDI to investigate the relationship between applied current amplitude and measured current density

Manuscript received April 23, 2009. This work was supported in part by the Henry M. Jackson Foundation for the Advancement of Military Medicine, Inc. under Contract 187733.

T. P. DeMonte is with Field Metrica Inc., Toronto, ON M8V 1W1 Canada (phone: 416-259-9842; e-mail: tdmonte@fieldmetrica.com).

D. Wang is with the Institute of Biomaterials and Biomedical Engineering, University of Toronto, Toronto, ON M5S 3G9 Canada (e-mail: dinghui.wang@utoronto.ca).

W. Ma is with the Institute of Biomaterials and Biomedical Engineering, University of Toronto, Toronto, ON M5S 3G9 Canada (e-mail: weijing.ma@utoronto.ca).

J-H. Gao is with Department of Radiology, University of Chicago, Chicago, IL 60637 USA (e-mail: jgao@radiology.bsd.uchicago.edu).

M. L. Joy is with the Institute of Biomaterials and Biomedical Engineering, University of Toronto, Toronto, ON M5S 3G9 Canada (e-mail: mikejoy@ecf.utoronto.ca).

magnitude in the range of 10 mA to 110 mA.

This recent study builds on previous work [3, 4] with the following improvements: A higher voltage current amplifier has been implemented to cover a greater range of applied current amplitudes over a greater range of electrode-tissue impedances. An improved method of holding electrodes against the skin reduces the problem of electrodes breaking away from the skin due to electrolysis and muscle twitch. Application of current pulses immediately following the R-wave of the cardiac cycle allows for high energy pulses to be applied without disrupting cardiac rhythm. The method of selecting highest quality measurements has been improved and will be discussed in the *Methods* section. All of these improvements have collectively resulted in better experimental technique yielding higher quality measurements over a greater range of applied current amplitude.

## II. METHODS

### A. Experimental Setup and Method

Piglets weighing 4 to 5 kg were anesthetized and placed in a frame that can be rotated into several positions within the MRI magnet. The CDI technique used in this work requires three orthogonal positions of the subject. The piglet was ventilated and injected with pancuronium (Pavulon®) to reduce muscle twitch. ECG electrodes were attached to three legs for monitoring. The MRI compatible SAI® ECG monitoring system includes a FORT module, triggered by the ECG gating signal, for blanking the ECG amplifier during application of current pulses as shown in fig. 1. Two circular 25.4 mm diameter copper electrodes with center-to-center spacing of 65 mm were placed on the chest of the piglet for applying current pulses using the CDI pulse generator hardware. Current pulses were passed through a radio frequency (RF) blocking filter to block MRI RF energy from interfering with the pulse generator hardware. Current pulses were also passed through a 3D CDI calibration module to ensure measurement quality. The ECG gating module triggers a pulse train generator which in turn triggers the MRI pulse sequence generator. Finally, the MRI pulse sequence generator triggers the CDI pulse generator to ensure synchronization of applied current.

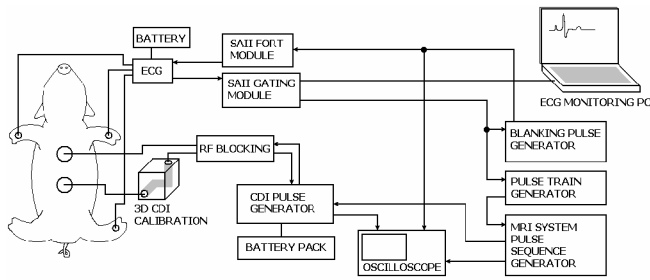


Fig. 1: Block diagram of experimental setup.

The MRI pulse sequence is a 3D fast gradient recalled echo sequence modified for CDI acquisitions with the pulse sequence shown in [3]. The repetition time (TR) for the MRI sequence was set to 8.32 ms and 16 lines of k-space were acquired with each heart beat. The MRI body coil was used to acquire 64 slices with 128 by 128 encoding steps. Field of view (FOV) was set to 48 cm resulting in a voxel size of 3.8 mm<sup>3</sup>. The MRI flip angle was set to 15 degrees and the bandwidth was set to +/-31.25 kHz. The square current pulses were 4.7 ms in duration with amplitudes ranging from 10 mA (47 μC charge) to 110 mA (517 μC charge). By comparison, TASER® main lobe pulse charges are estimated at 80 μC for the M26 model and 100 μC for the X26 model for a 1 kΩ resistive load.

Current pulse electrodes were held in place using an acrylic fixture that maintains a fixed distance between the electrodes (65 mm center-to-center). Adhesive conductive gel pads of about 1 mm thickness were placed between the copper electrodes and skin. The skin was shaved and abraded to increase conductivity. The fixture was held against the chest using nylon straps attached to the frame that holds the piglet. This method of holding electrodes against the skin is superior to previous methods that only use adhesives.

Between the R-wave and T-wave of an ECG signal, cardiac cells are mostly in a refractory state whereby they cannot be stimulated. This is the optimal time to apply current pulses because the pulses are unlikely to disrupt the cardiac rhythm. This time period is not the optimal time to acquire MRI data because there is contraction of cardiac muscles resulting in motion artifacts. For the purpose of this work, it was decided to optimize on the delivery of current pulses rather than minimization of cardiac motion artifacts.

### B. Methods of Data Processing and Analysis

Piglets were rotated into 3 orthogonal positions to measure the complete magnetic field generated by current pulses, as described in [1]. Magnetic field measurements were processed to compute current density vectors using the differential form of Ampere's law

$$\vec{J} = \nabla \times \vec{H} \quad (1)$$

Vector plots and streamlines were computed using the

MayaVi data visualization software [5].

The CDI technique inherits artifacts associated with MRI plus a few artifacts that are unique to CDI [6, 7]. Due to these artifacts, some measurements of current density are poor in quality. Rather than resolving these artifacts, this work applies various methods of identifying poor quality measurements and removing them. Fig. 2 shows the results of applying various methods of determining the quality of CDI measurements and combining these methods to locate the highest quality measurements. Fig 2(a) shows an iso-surface of the piglet constructed from anatomical MRI data. Fig 2(b) shows the same data in fig. 2(a) with transparent surface rendering elements such that one can “see through” the anatomy. Fig 2(c) shows the highest quality voxels (i.e. current density measurements at various points in space) in red colour as determined by the MRI signal-to-noise ratio (SNR). Current density measurements associated with MRI acquisitions below some specified threshold SNR (approximately MRI SNR < 3) are considered to be low quality and are discarded. Fig. 2(d) shows the highest quality voxels in green colour as determined by distance from the magnetic center of the MRI system. MRI systems exhibit geometric distortions related to nonlinear gradient fields. This artifact is zero at the magnetic center and increases with the distance from the magnetic center (a nonlinear relationship usually monotonic increasing). A radius of 68 mm from the magnetic center was selected as a threshold for determining good quality CDI measurements. The spherical region in fig. 2(d) shows this region of good quality measurements. Fig. 2(e) shows highest quality voxels in blue colour as determined from a current density magnitude outlier threshold. Some threshold (in the range of 15 to 60 A/m<sup>2</sup>) was selected for each individual experiment as an upper limit of reasonable measurement values. Fig. 2(f) shows highest quality voxels in yellow colour as determined from current density vector angle outlier threshold. For a series of experiments, the variance (i.e. standard deviation squared) of the two vector angles associated with spherical coordinates (theta and phi) were determined. Current density measurements exhibiting an angular variance of greater than 18 degrees were discarded. Fig. 2(g) shows the combination of all quality determination methods. The binary masks for all methods were bitwise ANDed and applied to the current density voxels to remove all poor quality measurements. Fig. 2(h) shows the remaining voxels representing the highest quality current density measurements. Table 1 gives a summary of the quality determination methods and the number of voxels remaining in each associated binary mask for one series of experiments that applied current pulse amplitudes at 10, 20, 30, 40, 50, 60, 70 and 80 mA. The final step of data analysis is to average together the magnitudes of the remaining high quality current density measurements. The number of measurements averaged together varies for each series of experiments and is typically several hundred voxels.

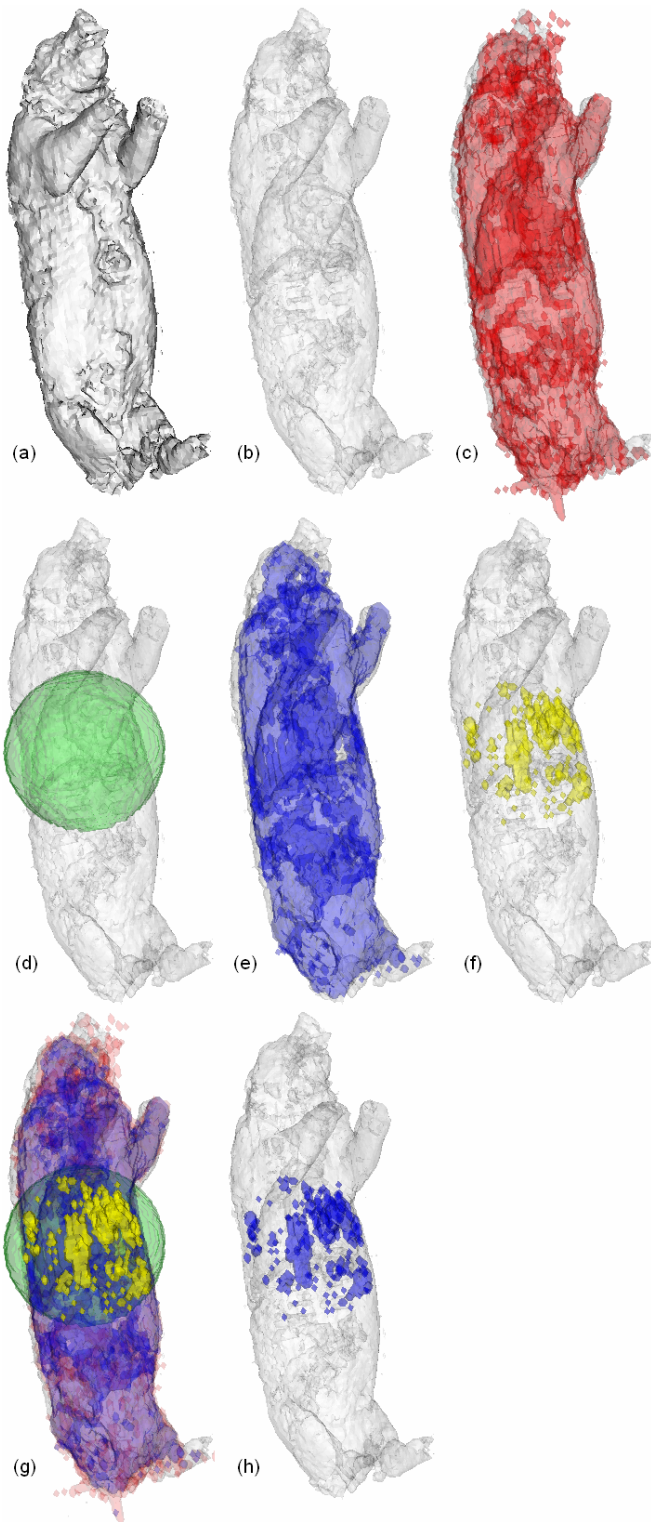


Fig. 2: (a) Iso-surface of piglet based on anatomical MRI. (b) Same as (a) with transparent rendering. (c) Red voxels have MRI SNR > 3. (d) Green voxels are within 68 mm radius of MRI magnetic center. (e) Blue voxels are below a reasonable upper limit of current density magnitude. (f) Yellow voxels have vector angle variances within 18 degrees across a series of experiments. (g) All selected voxels are combined by bitwise ANDING all binary masks. (h) Resulting group of current density measurements that are considered to be of highest quality.

TABLE I  
NUMBER OF HIGH QUALITY MEASUREMENTS REMAINING  
AFTER EACH QUALITY TEST

Quality Test Method	Figure	Number of High Quality Values Remaining
MRI SNR > 3	Fig. 2(c)	35146
Within radius of 68 mm from magnetic center	Fig. 2(d)	24464
Current density magnitude less than reasonable upper limit.	Fig. 2(e)	25908
Current density vector angles within variance of 18 degrees	Fig. 2(f)	1006
Combining all of the above quality tests	Fig. 2(g) and 2(h)	568

### III. RESULTS

Once current density vectors are computed, the current pathways through the torso can be visualized as shown in fig. 3. In fig. 3, green arrows represent a vector plot of current density vectors in one selected plane; red curves show some possible streamlines that were computed from the vector data indicating pathways of current through the heart and torso; and blue circles (or ellipses in fig. 3(c)) show the positions of electrodes on the chest. Fig. 3(a) is a close up of the chest view showing the heart, lungs and diaphragm. Fig. 3(b) is the same view as fig. 3(a) showing the whole body of the piglet. Fig. 3(c) is a left-side view of the whole body showing that the streamlines follow 3D pathways through the tissue.

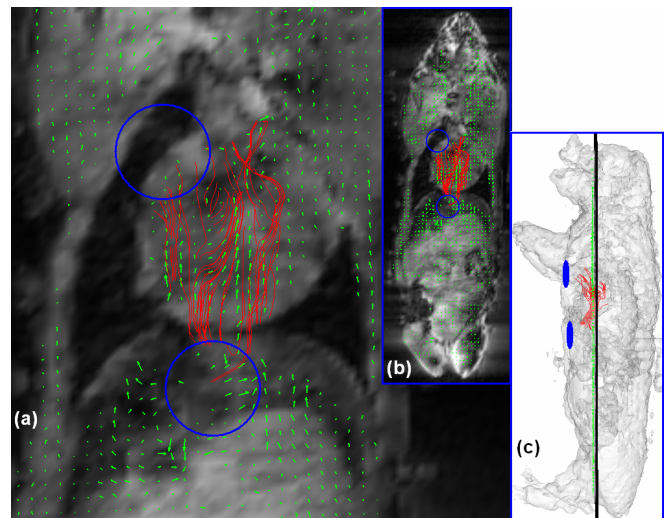


Fig. 3: CDI vector plot shown as green arrows superimposed on structural anatomical MRI data. (a) Chest view showing heart, lungs and diaphragm at a cross-section shown by the black line in the left side view of (c). Blue circles indicate positions of electrodes on the chest. (b) Full body view of (a). (c) Left-side view.

The highest quality current density measurements are determined using the methods described in the previous section for three series of experiments. The first experiment series (Experiment #1) includes current density

measurements with applied current amplitudes of 10, 20, 30, 40, 50, 60, 70 and 80 mA. The second experiment series (Experiment #2) includes measurements with applied current amplitudes of 70, 80, 90 and 100 mA. The third experiment series (Experiment #3) includes current amplitudes of 20, 30, 50, 70, 80, 90 and 110 mA. The average value of current density magnitude is plotted against applied current amplitude in fig. 4 for all three experiment series.

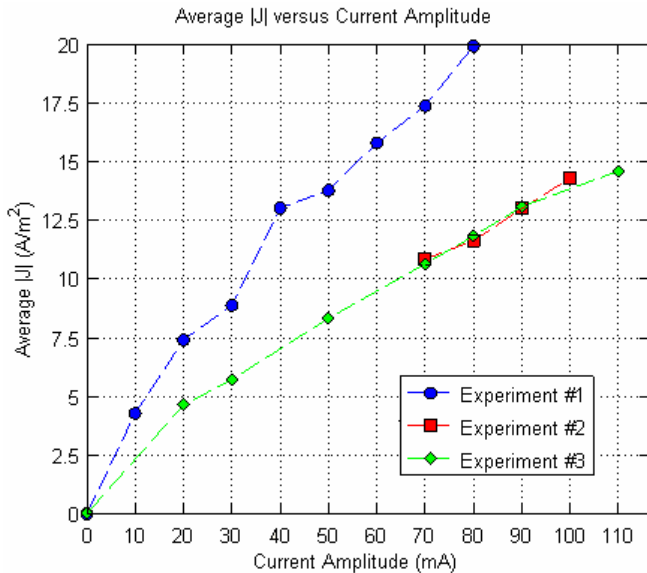


Fig. 4: Average current density magnitude versus applied current amplitude for three series of experiments.

#### IV. DISCUSSION

One of the major improvements shown in this work over previous work by this lab [3, 4] on the topic of current amplitude versus current density magnitude is the methods of selecting high quality measurements. Comparing fig. 3(f) with fig. 3(h) shows that the method of determining quality based on the variance of vector angles is the most constraining method resulting in only several hundred remaining measurements. This observation indicates that this method could potentially be applied as the only method and lead to similar results. However, the other methods have importance based on their theoretical foundations and they do collectively remove hundreds more measurements that fail to meet quality criteria.

The data from experiment #1 appears at a different scaling from experiments #2 and #3 because each experiment selects a different number of measurements considered as highest quality. Experiments #2 and #3 exhibit similar scaling by chance. From the graph of fig. 4, it is evident that the relationship between applied current amplitude and measured current density magnitude over the range of 10 mA to 110 mA is not quite linear. For a perfectly linear relationship, it is expected that the line in the graph would exhibit a zero intercept which is clearly not the case for these

measurements. These results indicate a bend in the curve around 20 to 30 mA. It is likely that tissues exhibit some nonlinearity, with respect to applied current amplitude, in their electrical properties, i.e. conductivity and permittivity. This is imaginable given the chemical complexity of tissue compared to simple electronic elements such as wires and resistors. Previous results from this lab [3, 4] indicated a more linear relationship, but these measurements were made over smaller ranges of applied amplitudes and the methods of determining high quality measurements were not as well developed.

Another important result from this work is the fact that within a time span of about 15 minutes, millions of current pulses exceeding a charge of 500  $\mu\text{C}$  could be applied to the chest of a small piglet (4 to 5 kg) near the heart without fatally disrupting cardiac function under the condition that these pulses are applied within a window of about 180 ms following the R-wave of the cardiac cycle (typical heart rate is about 100 BPM). The mechanism relied on here is the refractory period of cardiac cells. Other experiments in this lab have shown that cardiac function can be disrupted by current pulses with charge as low as 190  $\mu\text{C}$  when these pulses are applied following the T-wave of the cardiac cycle. These observations can potentially be used to develop a safer HEMI device. A limitation of present HEMI devices is that they apply electrical shocks without information regarding the cardiac cycle (i.e. ECG measurement). This consideration of HEMI device design has been previously acknowledged by other researchers, for example [8].

#### REFERENCES

- [1] G. C. Scott, M. L. G. Joy, R. L. Armstrong, R. M. Henkelman. Measurement of nonuniform current density by magnetic resonance. *IEEE Trans. Med. Imag.*, Vol. 10, No. 3, pp. 362-374, 1991.
- [2] Richard S. Yoon, Tim P. DeMonte, Karshi F. Hasanov, Dawn B. Jorgenson, and Michael L.G. Joy. Measurement of Thoracic Current Flow in Pigs for the Study of Defibrillation and Cardioversion. *IEEE Trans. Biomed. Eng.*, Vol. 50, No. 10, October 2003.
- [3] Tim P. DeMonte, Jia-Hong Gao, Dinghui Wang, Weijing Ma, and Michael L.G. Joy, "Measurement of Current Density Vectors in a Live Pig for the Study of Human Electro-muscular Incapacitation Devices", in *Proc. 30th Annu IEEE Int. Conf. EMBS*, Vancouver, 2008.
- [4] Tim P. DeMonte, Jia-Hong Gao, Dinghui Wang, Weijing Ma, and Michael L. Joy, "Investigation of Relationship between Applied Current Amplitude and Measured Current Density Magnitude in a Live Pig", in *Proc. 16th Annu. ISMRM Int. Conf.*, Toronto, 2008.
- [5] P. Ramachandran. The MayaVi Data Visualizer, Available: <http://mayavi.sourceforge.net/>.
- [6] G. C. Scott, M. L. G. Joy, R. L. Armstrong, and R. M. Henkelman. Sensitivity of Magnetic Resonance Current Density Imaging. *J. Mag. Res.*, 97, pp. 235-254, 1992.
- [7] T.P. DeMonte, R.S. Yoon, D. Jorgenson, and M.L.G. Joy, "Artifacts Associated with Measuring Cardiac Electrical Currents in a Post-mortem Pig Using Current Density Imaging", in *Proc. 10th Annu. ISMRM Int. Conf.*, Hawaii, 2002.
- [8] Robert A. Stratbucker, "Safe and efficient electrically based intentional incapacitation device comprising biofeedback means to improve performance and lower risk to subjects," U.S. Patent 6 898 887, May 31, 2005.